

Superconductivity in a new layered nickel-selenide CsNi_2Se_2

Huimin Chen,¹ Jinhu Yang,¹ Chao Cao,¹ Lin Li,¹ Qiping Su,¹ Bin Chen,¹
Hangdong Wang,^{1,2,*} Qianhui Mao,² Jianhua Du,² and Minghu Fang^{2,3,†}

¹Hangzhou Key Laboratory of Quantum Matter, Department of Physics,
Hangzhou Normal University, Hangzhou 310036, China

²Department of Physics, Zhejiang University, Hangzhou 310027, China

³Collaborative Innovation Center of Advanced Microstructures, Nanjing 210093, China

(Dated: August 24, 2015)

The physical properties of CsNi_2Se_2 were characterized by electrical resistivity, magnetization and specific heat measurements. We found that the stoichiometric CsNi_2Se_2 compound undergoes a superconducting transition at $T_c=2.7\text{K}$. A large Sommerfeld coefficient γ_n ($\sim 77.90 \text{ mJ/mol}\cdot\text{K}^{-2}$), was obtained from the normal state electronic specific heat. However, the Kadowaki-Woods ratio of CsNi_2Se_2 was estimated to be about $0.041 \times 10^{-5} \mu\Omega\cdot\text{cm}(\text{mol}\cdot\text{K}^2/\text{mJ})^2$, indicating the absence of strong electron-electron correlations. In the superconducting state, we found that the zero-field electronic specific heat data, $C_{es}(T)$ ($0.5\text{K} \leq T < 2.6\text{K}$), can be well fitted with a two-gap BCS model, indicating the multi-gap feature of CsNi_2Se_2 . In the end, the comparison with the density functional theory (DFT) calculations suggested that the large γ_n in these nickel-selenide superconductors may be related to the large Density of States (DOS) at the fermi surface.

PACS numbers: 74.62.Bf; 74.25.Op; 74.25.F-

After the discovery of the iron-based superconductors, people are exploring in the similar layered compounds where the Fe ions are replaced by the other 3d metal ions, in order to discover the next-generation of high- T_c superconductors and provide new opportunities for solid-state physics. NiPn-based (Pn: pnictogen) compounds are considered to be promising candidate for new superconductors, as the superconductivity has been observed in LaNiPO ($T_c \sim 3 \text{ K}$) [1], LaNiAsO ($T_c \sim 2.75 \text{ K}$) [2], BaNi_2As_2 ($T_c \sim 0.7 \text{ K}$) [3], BaNi_2P_2 ($T_c \sim 2.4 \text{ K}$) [4], SrNi_2P_2 ($T_c \sim 1.4 \text{ K}$) [5], and so on. However, the superconductivity in Ni-chalcogenide is rarely reported.

Recently, KNi_2Se_2 [6] and KNi_2S_2 [7], which have a similar structure to the iron-based superconductors $\text{A}_y\text{Fe}_{2-x}\text{Se}_2$ ($\text{A}=\text{Tl, K, Rb, Cs}$) [8, 9], were reported to be superconductivity with $T_c \sim 0.8\text{K}$ and $\sim 0.4\text{K}$, respectively. Upon replacement of the K with Tl, the transition temperature even can rise to be 3.7K for TlNi_2Se_2 [10]. Compared with $\text{A}_y\text{Fe}_{2-x}\text{Se}_2$ ($\text{A}=\text{Tl, K, Rb, Cs}$), it is homogenous without Ni vacancy in TlNi_2Se_2 , suggesting a heavy electron doping on the fermi surface. Interestingly, no superconducting transition was observed in the unstoichiometric compound $\text{K}_{0.95}\text{Ni}_{1.86}\text{Se}_2$ (may equal to the hole doping) down to 0.3K [11], even the physical properties were very similar with that of the stoichiometric KNi_2Se_2 . For these Ni-chalcogenide superconductors, the superconductivity usually appears to involve heavy electrons [6, 7, 10], as inferred from the large Sommerfeld coefficient, γ_n . This result may make them be a bridge between cuprate- or iron-based and conventional heavy-fermion superconductors. By now, the origin of the large γ_n at low temperature is not confirmed yet. An intriguing possibility is that the large γ_n is due to the existence of local charge order, which may induce the strong elec-

tron correlations and heavy-fermion behavior [6, 7, 10]. However, the recent angle-resolved photoemission spectroscopy (ARPES) and optical spectroscopy studies reveal the weak correlation feature in these Ni-chalcogenide superconductors. Instead, they suggested that the large γ_n may be ascribed to the large density states and the Van Hove singularity in the vicinity of the fermi energy [12–14].

Though the Ni-chalcogenide superconductors have been studied for several years, the superconductivity in the single crystalline sample had only been realized in TlNi_2Se_2 [10] and TlNi_2S_2 [15] by now. To understand the intrinsic properties, more superconducting samples, especially the alkali metal compounds, are needed to be investigated. In this paper, we synthesized the CsNi_2Se_2 single crystal successfully. The measurements of resistivity, magnetization and specific heat were carried out down to $T=0.5\text{K}$. It was found that the stoichiometric CsNi_2Se_2 compound undergoes a superconducting transition at $T_{c\text{onset}}=2.7\text{K}$, which is very different from that in $\text{K}_{0.95}\text{Ni}_{1.86}\text{Se}_2$ single crystal [11]. At low temperatures, a large Sommerfeld coefficient, γ_n ($\sim 77.90 \text{ mJ/mol}\cdot\text{K}^2$), was obtained from the normal state electronic specific heat. In the superconducting state, we found that the zero-field electronic specific heat data, $C_{es}(T)$ ($0.5\text{K} \leq T < 2.6\text{K}$), can be well fitted using a two-gap BCS model, indicating the multi-gap feature of CsNi_2Se_2 . At the end, density functional theory (DFT) calculations were performed for TlNi_2Se_2 , KNi_2Se_2 and CsNi_2Se_2 , respectively, and the result was compared with their corresponding large γ_n . It suggested that the large γ_n may be related to the large DOS at the Fermi surface in these nickel-selenide superconductors.

Large plate-like single crystals of CsNi_2Se_2 were grown

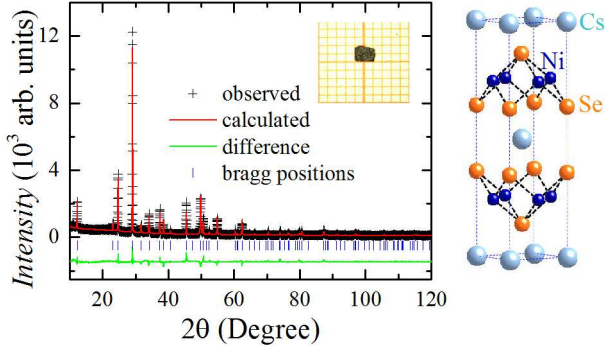


FIG. 1: (Color online) Left: Rietveld refinement profile for the powder x-ray diffraction of CsNi_2Se_2 . Right: Crystal structure of stoichiometric CsNi_2Se_2 with the tetragonal ThCr_2Si_2 -type structure. Inset: A photo of CsNi_2Se_2 crystal.

using self-flux method. First, the precursor Cs_2Se was prepared by heating Cs and Se powders at 200°C . Then, Cs_2Se , Ni and Se powders were mixed in an appropriate stoichiometry and were put into alumina crucibles and sealed in an evacuated silica tube. The mixture was heated up to 1000°C and kept over 3 hours. Then the melting mixture was cooled down to 700°C in a cooling rate of $3^\circ\text{C}/\text{h}$. Finally the furnace was cooled to room temperature after shutting down the power. The structure of single crystals was characterized by X-ray diffraction (XRD). To avoid exposure to air, the sample was sealed using *N*-grace during the XRD data collecting. In the powder XRD patterns (figure 1), all peaks can be well indexed with a ThCr_2Si_2 -type structure (space group: $I4/mmm$). The lattice parameters, $a = 3.988\text{\AA}$, and $c = 14.419\text{\AA}$ were obtained by fitting the XRD data, indicating a larger unit cell than that of KNi_2Se_2 and TiNi_2Se_2 . The elemental analysis was performed using an energy-dispersive x-ray spectroscopy (EDX) in a Zeiss Supra 55 scanning electron microscope. The EDX results indicate that the crystals are rather homogenous and the determined average atomic ratios are $\text{Cs}:\text{Ni}:\text{Se} = 1.02:2.03:2.00$ when fixing Se stoichiometry to be 2, confirming the stoichiometry of CsNi_2Se_2 . The *ab*-plane $\rho(T)$ measurements were performed by the standard four-probe technique using the *Quantum Design* Physical Properties Measurement System PPMS-9. Temperatures down to 0.5 K were obtained using a ^3He attachment to the PPMS. The heat capacity measurements were carried out using the relaxation method. The magnetic susceptibility was measured using the *Quantum Design* MPMS-SQUID.

Figure 2(a) shows the electrical resistivity in the *ab*-plane, $\rho_{ab}(T)$, as a function of temperature for CsNi_2Se_2 crystal. The value of $\rho_{ab}(300\text{K})$ and $\rho_c(300\text{K})$ (not shown here) is about $204\mu\Omega\cdot\text{cm}$ and $572\mu\Omega\cdot\text{cm}$, respectively. Then the ρ_c/ρ_{ab} is calculated to be 2.8, indicating the anisotropy is not so large, although CsNi_2Se_2 owns a layered structure. Upon cooling down from room temperature, $\rho_{ab}(T)$ exhibits a metallic behavior. In the normal

state, no abnormal change in $\rho_{ab}(T)$ was observed, which occurs in both iso-structural BaNi_2As_2 [3] and SrNi_2P_2 [5] compounds, corresponding to the structural transition from a tetragonal at higher temperatures to a triclinic at lower temperatures. Below $T_c \sim 2.7\text{K}$, the $\rho_{ab}(T)$ drops to zero abruptly, suggesting a superconducting transition happens. It is also confirmed by a large diamagnetic signal [see the inset (iii) of figure 2] and a specific heat jump at T_c as shown in figure 2(d). The residual resistivity ratio [$\text{RRR} = \rho_{ab}(300\text{K})/\rho_{ab}(3\text{K}) \sim 37$] and superconducting transition width $\Delta T_c \sim 0.1\text{ K}$ reflects the high quality of the single crystals. At low temperatures ($3\text{K} \leq T \leq 20\text{K}$), it was found that the $\rho_{ab}(T)$ can be well fitted using the equation $\rho_{ab}(T) = \rho_0 + AT^2$, where $\rho_0 = 5.368\mu\Omega\cdot\text{cm}$ and $A = 2.474 \times 10^{-3}\mu\Omega\cdot\text{cm}/\text{K}^2$, suggesting a Fermi liquid ground state. Combining the value of Sommerfeld coefficient γ_n below, the Kadowaki-Woods ratio, A/γ^2 , was estimated to be $0.041 \times 10^{-5}\mu\Omega\cdot\text{cm}(\text{mol}\cdot\text{K}^2/\text{mJ})^2$. This value is one order of magnitude smaller than that for the standard heavy-fermion systems ($\sim 10^{-5}\mu\Omega\cdot\text{cm}(\text{mol}\cdot\text{K}^2/\text{mJ})^2$), and is quite similar with that for many transition metals ($\sim 0.04 \times 10^{-5}\mu\Omega\cdot\text{cm}(\text{mol}\cdot\text{K}^2/\text{mJ})^2$) [17, 18]. We suggest that this result may indicate the absence of strong correlation in this compound, which is consistent with the previous results [12–14].

Figure 2(b) is the field dependence of the $\rho_{ab}(T)$ of CsNi_2Se_2 at low temperatures, when the magnetic field was applied parallel to the *c* axis. The transition temperature T_c shifts to lower temperature in external magnetic fields. Using the middle superconducting transition temperature in $\rho_{ab}(T)$, the upper critical field H_{c2} is plotted as a function of temperature in the inset (ii) of figure 2(b). According to the Ginzburg-Landau theory, the zero temperature upper critical field $H_{c2}(0)$ can be estimated by using the formula $H_{c2}(T) = H_{c2}(0)(1 - t^2)/(1 + t^2)$, where t is the reduced temperature $t = T/T_c$. The fitting result yields the value of $\mu_0 H_{c2}(0) = 2\text{ Tesla}$, which is 2.5 times that of TiNi_2Se_2 [10]. The superconducting coherence length ξ_0 can be estimated from the relation $\xi_0 = [\Phi_0/2\pi H_{c2}]^{0.5}$, yielding $\xi_0^{ab} = 12.8\text{ nm}$. The normal state magnetic susceptibility, $\chi_{ab}(T)$, for CsNi_2Se_2 crystal, is plotted as a function of temperature in figure 2(c). It seems nearly temperature independent at high temperatures, consistent with previous reports of Pauli paramagnetism [16]. At low temperatures, it exhibits a Curie-tail like behavior, which may be due to the existence of magnetic impurity (as shown as the fitting blue line in figure 2(b) corresponding to $< 1.00\text{ mol \%}$ of an $S=1$ impurity, *e.g.* Ni^{2+}). However, we can't exclude the effect of spin fluctuation at low temperatures, which may play an important role in the superconductivity.

In the nickel-chalcogenide superconductors, the superconducting transitions always accompany a large Sommerfeld coefficient γ_n at low temperature, which may imply the non-trivial pairing mechanism. So we carried

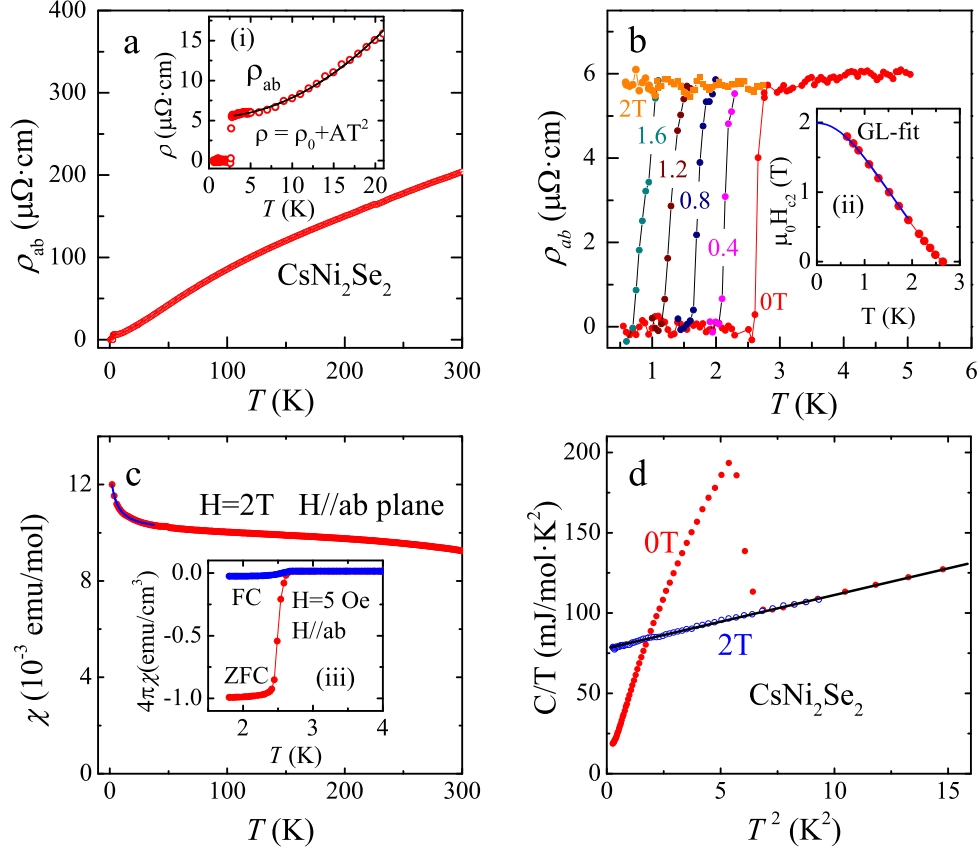


FIG. 2: (Color online) (a) Temperature dependence of *in*-plane resistivity, $\rho_{ab}(T)$ for CsNi₂Se₂ crystal. (b) The evolution of the in-plane resistivity $\rho_{ab}(T)$ under magnetic fields up to 2.0 T applied parallel to the *c* axis. (c) Temperature dependence of the normal state magnetic susceptibility, $\chi(T)$, measured at 2 Tesla field parallel to *ab* plane. (d) Specific heat divided by temperature, C/T vs. T^2 , measured under 0 and 2 T fields. The solid straight line is a guide to the eye. Inset: (i) $\rho_{ab}(T)$ near the superconducting transition; (ii) Upper critical field H_{c2} vs. T for CsNi₂Se₂ crystal. (iii) $\chi(T)$ near the superconducting transition, measured at 5 Oe field parallel to *ab* plane (for minimizing the demagnetization factor) with both zero-field cooling (ZFC) and field cooling (FC) processes.

out detailed measurements of the specific heat $C(T, H)$ for CsNi₂Se₂ crystal. Figure 2(d) shows the $C(T, H)/T$ as a function of T^2 , measured under 0 T, and 2 T field, respectively. For the normal state specific heat $C_N(T)$, a linear fit of the data from 0.5 K to 8 K to $C/T = \gamma + \beta T^2$ gives $\gamma = 77.90 \text{ mJ/mol} \cdot \text{K}^{-2}$ and $\beta = 3.32 \text{ mJ/mol} \cdot \text{K}^{-4}$, which implies a Debye temperature Θ_D of 139 K. Compared with the value of KNi₂Se₂ ($\sim 44 \text{ mJ/mol} \cdot \text{K}^{-2}$) [6] and TlNi₂Se₂ ($\sim 40 \text{ mJ/mol} \cdot \text{K}^{-2}$) [10], the Sommerfeld coefficient γ_n for CsNi₂Se₂ is much larger. It can even be compared with that for KFe₂As₂ ($\sim 94 \text{ mJ/mol} \cdot \text{K}^{-2}$), which is widely accepted as an unconventional superconductor [19].

The electronic specific heat ($C_{es}(T)$) in the superconducting state is obtained by the deduction of phonon contribution (βT^3) from the total $C(T)$. As shown in the figure 3(a), the normalized specific heat jump at T_c ($\Delta C/(\gamma_n T_c)$) is about 1.44, consistent with the theoretical value (1.43) of the well-known BCS theory. Then, we analyze the data by fitting $C_{es}(T)$ with different gap

functions. First, we consider the case of a single gap Δ_0 . The temperature dependence is taken to be the same as in the BCS theory, *i.e.* $\Delta(t) = \Delta_0 \delta(t)$, where $\delta(t)$ is the normalized BCS gap at the reduced temperature $t = T/T_c$ as tabulated by Mühlischlegel [20]. For a standard BCS-type superconductor, the thermodynamic properties, entropy (S) and C_{es} , can be written as:

$$S = -\frac{6\gamma_n \Delta_0}{\pi^2 k_B} \int_0^\infty [f \ln f + (1-f) \ln(1-f)] dy \quad (1)$$

$$C_{es} = T \frac{dS}{dT} \quad (2)$$

where $f = [\exp(\beta E) + 1]^{-1}$ and $\beta = (k_B T)^{-1}$. The energy of the quasi-particles is given by $E = [\varepsilon^2 + \Delta^2(t)]^{0.5}$, where ε is the energy of the normal electrons relative to the Fermi surface. The integration variable is $y = \varepsilon/\Delta_0$. Considering the multi-band feature of these nickel-chalcogenide superconductors as indicated in [12, 13, 21],

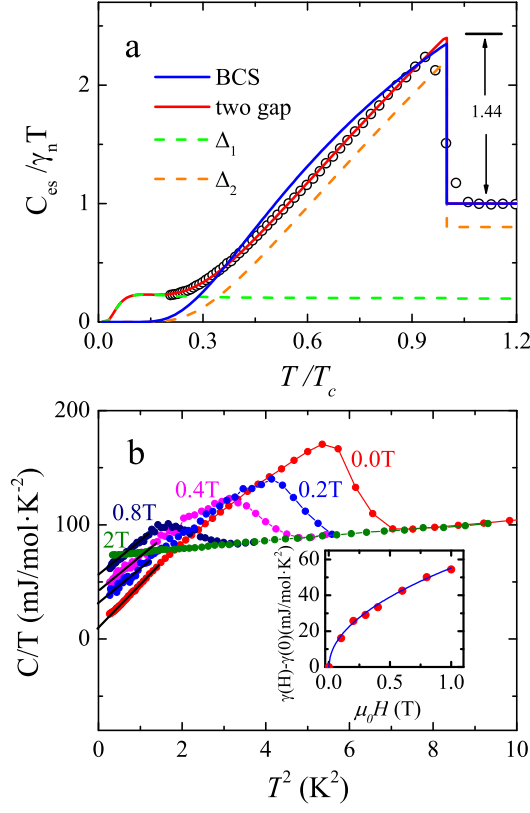


FIG. 3: (Color online) (a) Reduced temperature T/T_c dependence of electronic specific heat divided by temperature $C_{es}/\gamma T$ in the superconducting state at zero field, where $C_{es} = C - C_{latt}$. The two solid lines show the fitting curve of the conventional BCS model and the two-gap model to $C_{es}/\gamma T$, respectively. The two dashed lines show the individual contributions of the two gaps to $C_{es}/\gamma T$. (b) Low-temperature specific heat divided by temperature C/T vs. T^2 , measured at various fields near superconducting transition. Inset: Magnetic field dependence of field-induced electronic specific-heat coefficient $\Delta\gamma(H)$ in the mixed state.

we also carried out the fitting using two gap model, where the total specific heat can be considered as the sum of the contributions of each band calculated independently according to equations (1) and (2). It seems that the single-gap model fitting is not very good, especially at low temperatures, while the two-gap model presents the best fit to the C_{es}/T data [see figure 3a], just as described in [10]. In the figure 3a, we plot the contributions from the two superconducting gaps, $\Delta_1 = 0.22 k_B T_c$ and $\Delta_2 = 1.97 k_B T_c$, as well as their sum (red line). The weight contributed from the first gap, Δ_1 , is about 0.20.

To get more information of the superconducting gap, we also carried out the low temperature specific heat measurements under various magnetic fields, as shown in the figure 3b. At zero field, the linear extrapolation of C/T vs. T^2 to $T=0K$ gives a 'residual' Sommerfeld coefficient of $\gamma_0 = 5.5$ mJ/mol·K². Considering the air sensitive nature of CsNi₂Se₂, we may ascribe it to the ex-

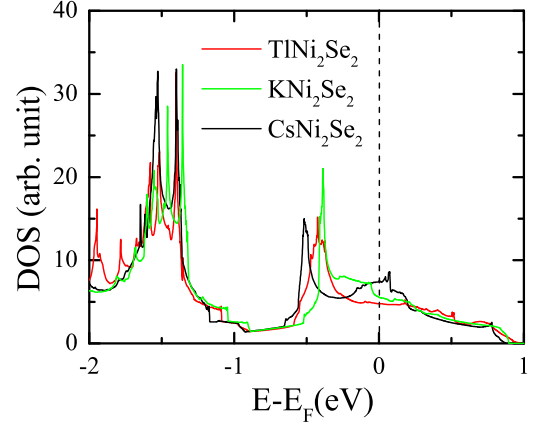


FIG. 4: (Color online) Partial DOS of KNi₂Se₂, TlNi₂Se₂, and CsNi₂Se₂ in the -2 to 1eV energy range relative to the Fermi energy. The dashed line is a guide to eyes.

istence of small fraction ($\sim 6.8\%$) of non-superconducting phase. With increasing of the magnetic field, the magnitude of the specific heat jump at T_c decreases, and the linear electronic specific heat coefficient, $\gamma(H)$, increases. In this study, the field dependence of $[\gamma(H) - \gamma(0)]$ obeys the Volovik relation (*i.e.*, $\propto H^{1/2}$) very well (the inset), just as observed in TlNi₂Se₂. This behavior was once considered as a common feature of the d-wave superconductors, where the $H^{1/2}$ term arises from a Doppler shift of the quasi-particle excitation spectrum in the outer regions of the vortices. Yet, this behavior may not be always so unique, because it was also observed in other s-wave superconductors, such as NbSe₂ [22, 23], V₃Si [24], and CeRu₂ [25]. Recently, low-temperature thermal conductivity measurements have identified the multiple nodeless superconducting gaps in TlNi₂Se₂ [26], so we suggest that the CsNi₂Se₂ may have the similar properties.

In the end, we present a roughly discussion about the origin of the large γ_n , by comparing TlNi₂Se₂, KNi₂Se₂ and CsNi₂Se₂ as typical cases, since they have the similar structure and almost same ions except the alkali metal (or thallium) ion. As mentioned above, the Sommerfeld coefficient γ_n for TlNi₂Se₂, KNi₂Se₂ and CsNi₂Se₂ are about 40, 44, and 79 mJ/mol·K², respectively. Usually, the large γ_n is related to the strong electron correlation. However, the ARPES and optical results have demonstrated the weak correlation in KNi₂Se₂ and TlNi₂Se₂ [12–14]. As well known, the γ_n is proportional to the DOS at E_F in a free electron framework. So we performed the DFT calculations for these three compounds (figure 4) to examine the relation between their DOS at E_F and γ_n . As shown in the figure, the DOS of all the three compounds exhibit a similar dispersion, indicating that they may contain similar electronic structure. At fermi energy, the DOS value increases in the order of TlNi₂Se₂, KNi₂Se₂ and CsNi₂Se₂. Furthermore, the es-

timated ratio of the DOS value in TiNi_2Se_2 , KNi_2Se_2 , and CsNi_2Se_2 is about 1 : 1.16 : 1.7, which is generally consistent with the corresponding ratio (1 : 1.1 : 1.95) of their γ_n . Therefore, we suggest that the large γ_n may be related to the large DOS at the Fermi surface in these nickel-selenide superconductors, which has also been proposed in [12] from another point of view.

In summary, we synthesized the CsNi_2Se_2 single crystal successfully. The measurements of resistivity, magnetization and specific heat were carried out down to $T=0.5\text{K}$. It was found that the stoichiometric CsNi_2Se_2 compound undergoes a superconducting transition at $T_c^{\text{onset}}=2.7\text{K}$. A large Sommerfeld coefficient, γ_n ($\sim 77.90\text{ mJ/mol}\cdot\text{K}^{-2}$), was obtained from the normal state electronic specific heat. However, the Kadowaki-Woods ratio of CsNi_2Se_2 was estimated to be about $0.041 \times 10^{-5} \mu\Omega\cdot\text{cm}(\text{mol}\cdot\text{K}^2/\text{mJ})^2$, comparable with those for transition metals, which may indicate the absence of strong electron-electron correlation. In the superconducting state, we found that the zero-field electronic specific heat data, $C_{es}(T)$ ($0.5\text{K} \leq T < 2.6\text{K}$), can be well fitted with a two-gap BCS model, indicating the multi-gap feature of CsNi_2Se_2 . At the end, density functional theory calculations were performed for TiNi_2Se_2 , KNi_2Se_2 and CsNi_2Se_2 , respectively. The result indicated that the ratio of the DOS value at E_F is generally consistent with the corresponding ratio of their γ_n , suggesting that the large γ_n may be related to the large DOS at the Fermi surface.

This work is supported by the National Basic Research Program of China (973 Program) under grant No. 2011CBA00103, 2012CB821404 and 2009CB929104, the Nature Science Foundation of China (Grant No. 10974175, 10934005, 11204059 and 11274006), and Zhejiang Provincial Natural Science Foundation of China (Grant No. LR12A04003), and the Fundamental Research Funds for the Central Universities of China.

* Electronic address: hdwang@hznu.edu.cn

† Electronic address: mhfang@zju.edu.cn

- [1] Watanabe T., Yanagi H., Kamiya T., Kamihara Y., Hiramatsu H., Hirano M. and Hosono H., *Inorg. Chem.* **46**, 7719(2007)
- [2] Li Z. *et al.*, *Phys. Rev. B* **78**, 060504(2008)

- [3] Ronning F. *et al.*, *J. Phys.: Condens. Matter* **20**, 342203(2008)
- [4] Tomioka Y., Ishida S., Nakajima M., Ito T., Kito H., Iyo A., Eisaki H. and Uchida S., *Phys. Rev. B* **79**, 132506(2009)
- [5] Ronning F. *et al.*, *Phys. Rev. B* **79**, 134507(2009)
- [6] Neilson J. R. *et al.*, *Phys. Rev. B* **85**, 054512(2012)
- [7] Neilson J. R., McQueen T. M., Llobet A., Wen J. J. and Suchomel M. R., *Phys. Rev. B* **87**, 045124(2013)
- [8] Guo J. G., Jin S. F., Wang G., Wang S. C., Zhu K. X., Zhou T. T., He M. and Chen X. L., *Phys. Rev. B* **82**, 180520(2010)
- [9] Fang M. H., Wang H. D., Dong C. H., Li Z. J., Feng C. M., Chen J. and Yuan H. Q., *Europhys. Lett.* **94**, 27009(2011)
- [10] Wang H. D., Dong C. H., Mao Q. H., Khan R., Zhou X., Li C. X., Chen B., Yang J. H., Su Q. P., and Fang M. H., *Phys. Rev. Lett.* **111**, 207001(2013)
- [11] Lei H. C., Abeykoon M., Wang K. F., Bozin E. S., Ryu H., Graf D., Warren J. B. and Petrovic C., *J. Phys.: Condens. Matter* **26**, 015701(2013)
- [12] Fan Q. *et al.*, *Phys. Rev. B* **91**, 125113(2015)
- [13] Xu N. *et al.*, arXiv:1412.7016
- [14] Wang X. B., Wang H. P., Wang H. D., Fang M. H. and Wang N. L., arXiv:1507.01690
- [15] Wang H. D., Mao Q. H., Chen H. M., Dong C. H., Khan R., Yang J. H., Chen B. and Fang M. H., arXiv:1305.1033
- [16] Huan G., Greenblatt M. and Croft M., *Eur. J. Solid State Inorg. Chem.* **26**, 193(1989)
- [17] Kadowaki K. and Woods S. B., *Solid State Commun.* **58**, 507(1986)
- [18] Jacko A. C., Fjærestad J. O. and Powell B. J., *Nat. Phys.* **5**, 422 (2009)
- [19] Abdel-Hafez M., Aswartham S., Wurmehl S., Grinenko V., Hess C., Drechsler S. L., Johnston S., Wolter A. U. B., Büchner B., Rosner H. and Boeri L., *Phys. Rev. B* **85**, 134533 (2012)
- [20] Mühlischlegel B., *Z. Phys.* **155**, 313 (1955)
- [21] Lu F., Wang W. H., Xie X. J. and Zhang F. C., *Phys. Rev. B* **87**, 115131(2013)
- [22] Sanchez D., Junod A., Muller J., Berger H. and Lévy F., *Physica (Amsterdam)* **204B**, 167(1995)
- [23] Sonier J. E., Hundley M. F., Thompson J. D. and Brill J. W., *Phys. Rev. Lett.* **82**, 4914(1999)
- [24] Ramirez A. P., *Phys. Lett. A* **211**, 59(1996)
- [25] Hedo M., Inada Y., Yamamoto E., Haga Y., Onuki Y., Aoki Y., Matsuda T.D., Sato H. and Takahashi S., *J. Phys. Soc. Jpn.* **61**, 272 (1998)
- [26] Hong X. C., Zhang Z., Zhou S. Y., Pan J., Xu Y., Wang H. D., Mao Q. H., Fang M. H., Dong J. K. and Li S. Y., *Phys. Rev. B* **90**, 060504 (2014)